

Self-consistent optical parameters of intrinsic silicon at 300 K including temperature coefficients

Martin A. Green*

ARC Photovoltaics Centre of Excellence, University of New South Wales, Sydney, NSW 2052, Australia

ARTICLE INFO

Article history:

Received 29 April 2008

Accepted 19 June 2008

Available online 25 July 2008

Keywords:

Absorption coefficient

Optical properties

Silicon solar cells

ABSTRACT

An updated tabulation is presented of the optical properties of intrinsic silicon, of particular interest in solar cell calculations. Improved values of absorption coefficient, refractive index and extinction coefficient at 300 K are tabulated over the 0.25–1.45 μm wavelength range at 0.01 μm intervals. The self-consistent tabulation was derived from Kramers–Kronig analysis of updated reflectance data deduced from the literature. The inclusion of normalised temperature coefficients allows extrapolation over a wide temperature range, with accuracy similar to that of available experimental data demonstrated over the -24°C to 200°C range.

© 2008 Elsevier B.V. All rights reserved.

1. Introduction

Accurate tabulations of silicon's optical properties are of use in calculations of silicon solar cell properties and in extracting cell parameters. Since two earlier versions of the present table [1,2], relevant developments include a review of silicon's optical properties over the 1.1–3.1 eV range [3], new ellipsometric measurements over the 0.75–6.5 eV range [4], investigation of a generalised Cauchy dispersion formula to model silicon's infrared index [5–7], and accurate measurement of silicon's sub-bandgap absorption coefficient using high-performance silicon LEDs [8] and photoluminescence from silicon wafers [9,10].

An updated tabulation of absorption coefficient, α , and the real and (negative) imaginary parts of the refractive index (n and k , respectively) is given in Table 1. The extinction coefficient, k , and α are directly related, $\alpha = 4\pi k/\lambda$, where λ is free-space wavelength (λ and energy, E , were converted using λ (μm) = 1.23984190/ E (eV), the most recent CODATA recommendation [11]; for standard dry air, wavelengths will be about 0.03% shorter [12]). Data are given at 300 K over the 0.25–1.45 μm range at 0.01 μm intervals, together with normalised temperature coefficients allowing use over an extended temperature range.

2. Methodology

A recent careful ellipsometric study of silicon's optical properties [4] gave results in disagreement with earlier studies [13–15],

as well as α and k values unlikely to be correct at low E . The challenge in preparing Table 1 was finding a self-consistent way to incorporate all such earlier work most effectively. Checking calculated values of reflectance, R , using different data sets, the relative R difference was often found to be smaller than corresponding relative differences in reported n and k .

The procedure, therefore, adopted was to use these earlier studies (plus other available data) to calculate an updated curve for reflectance versus photon energy. Following Philipp [14], the phase of R in radians, θ , can then be calculated at target energy, E_t , from Kramers–Kronig analysis. The relation used in the present work is [16]

$$\theta(E_t) = -\frac{E_t}{\pi} \left\{ \int_0^{E_t-\delta} \frac{\ln[R(E)]}{E^2 - E_t^2} dE + \int_{E_t+\delta}^{\infty} \frac{\ln[R(E)]}{E^2 - E_t^2} dE \right\} \quad (1)$$

where $\delta \rightarrow 0$ (E units arbitrary); n and k are then calculated as [16]

$$n(E) = \frac{1 - R(E)}{1 + R(E) - \sqrt{2R(E)} \cos \theta} \quad (2)$$

$$k(E) = \frac{2\sqrt{R(E)} \sin \theta}{1 + R(E) - 2\sqrt{R(E)} \cos \theta} \quad (3)$$

Silicon is shown to be well suited to such analysis due to the wide range of energies for which reflection data are available (from below 0.005 eV to above 29 keV) and its well-behaved behaviour beyond these energies.

* Tel.: +61 2 9385 4018.

E-mail address: m.green@unsw.edu.au

Table 1
Optical properties of intrinsic silicon at 300 K including normalised temperature coefficients

λ (μm)	α (/cm)	n	k	C_n ($10^{-4}/\text{K}$) ($1/n$) (dn/dt)	$C_{k,x}$ ($10^{-4}/\text{K}$) ($1/k$) (dk/dt)
0.25	1.84E6	1.665	3.665	2.9	-0.9
0.26	1.97E6	1.757	4.084	2	-1.5
0.27	2.18E6	2.068	4.680	0	-3.1
0.28	2.37E6	2.959	5.287	-4.8	-3.3
0.29	2.29E6	4.356	5.286	-9	0.8
0.3	1.77E6	4.976	4.234	-3.8	2.5
0.31	1.46E6	5.121	3.598	-1.6	3.2
0.32	1.30E6	5.112	3.303	-1.3	1.5
0.33	1.18E6	5.195	3.100	-1.2	0.7
0.34	1.10E6	5.301	2.977	-1	0.3
0.35	1.06E6	5.494	2.938	-1.8	0
0.36	1.04E6	6.026	2.966	-4.1	-1.4
0.37	7.37E5	6.891	2.171	-4.4	4.2
0.38	3.13E5	6.616	0.946	-2.3	9.1
0.39	1.43E5	6.039	0.445	1	26
0.4	9.30E4	5.613	0.296	2.1	33
0.41	6.95E4	5.330	0.227	2.1	31
0.42	5.27E4	5.119	0.176	1.9	29
0.43	4.02E4	4.949	0.138	1.8	29
0.44	3.07E4	4.812	0.107	1.7	28
0.45	2.41E4	4.691	0.086	1.6	28
0.46	1.95E4	4.587	0.071	1.6	29
0.47	1.66E4	4.497	0.062	1.5	29
0.48	1.44E4	4.419	0.055	1.4	30
0.49	1.26E4	4.350	0.049	1.4	30
0.5	1.11E4	4.294	0.044	1.3	31
0.51	9700	4.241	0.039	1.3	31
0.52	8800	4.193	0.036	1.2	32
0.53	7850	4.151	0.033	1.2	33
0.54	7050	4.112	0.030	1.2	33
0.55	6390	4.077	0.028	1.1	33
0.56	5780	4.045	0.026	1.1	34
0.57	5320	4.015	0.024	1.1	34
0.58	4880	3.988	0.023	1.1	34
0.59	4490	3.963	0.021	1	34
0.6	4175	3.940	0.020	1	34
0.61	3800	3.918	0.018	1	35
0.62	3520	3.898	0.017	1	35
0.63	3280	3.879	0.016	1	35
0.64	3030	3.861	0.015	1	35
0.65	2790	3.844	0.014	0.9	35
0.66	2570	3.828	0.013	0.9	35
0.67	2390	3.813	0.013	0.9	36
0.68	2200	3.798	0.012	0.9	36
0.69	2040	3.784	0.011	0.9	36
0.7	1890	3.772	0.011	0.9	37
0.71	1780	3.759	0.010	0.9	37
0.72	1680	3.748	0.010	0.9	37
0.73	1540	3.737	0.009	0.8	37
0.74	1420	3.727	0.008	0.8	37
0.75	1310	3.717	0.008	0.8	37
0.76	1190	3.708	0.007	0.8	37
0.77	1100	3.699	0.007	0.8	37
0.78	1030	3.691	0.006	0.8	37
0.79	928	3.683	0.006	0.8	38
0.8	850	3.675	0.005	0.8	40
0.81	775	3.668	0.005	0.8	41
0.82	707	3.661	0.005	0.8	42

Table 1 (continued)

λ (μm)	α (/cm)	n	k	C_n ($10^{-4}/\text{K}$) ($1/n$) (dn/dt)	$C_{k,\alpha}$ ($10^{-4}/\text{K}$) ($1/k$) (dk/dt)
0.83	647	3.654	0.004	0.7	44
0.84	590	3.647	0.004	0.7	45
0.85	534	3.641	0.004	0.7	46
0.86	479	3.635	0.003	0.7	47
0.87	431	3.630	0.003	0.7	49
0.88	383	3.624	0.003	0.7	51
0.89	343	3.619	0.002	0.7	52
0.9	303	3.614	0.002	0.7	54
0.91	271	3.609	0.002	0.7	56
0.92	240	3.604	0.002	0.7	57
0.93	209	3.600	0.002	0.7	59
0.94	183	3.595	0.001	0.7	62
0.95	156	3.591	0.001	0.7	65
0.96	134	3.587	0.001	0.7	69
0.97	113	3.583	0.001	0.7	73
0.98	96.0	3.579	0.001	0.7	78
0.99	79.0	3.575	0.001	0.7	83
1	64.0	3.572	0.001	0.7	90
1.01	51.1	3.568	–	0.7	97
1.02	39.9	3.565	–	0.7	105
1.03	30.2	3.562	–	0.7	112
1.04	22.6	3.559	–	0.6	120
1.05	16.3	3.556	–	0.6	135
1.06	11.1	3.553	–	0.6	145
1.07	8.0	3.550	–	0.6	155
1.08	6.2	3.547	–	0.6	160
1.09	4.7	3.545	–	0.6	165
1.1	3.5	3.542	–	0.6	175
1.11	2.7	3.540	–	0.6	180
1.12	2.0	3.537	–	0.6	185
1.13	1.5	3.535	–	0.6	190
1.14	1.0	3.532	–	0.6	200
1.15	0.68	3.530	–	0.6	210
1.16	0.42	3.528	–	0.6	230
1.17	0.22	3.526	–	0.6	260
1.18	6.5E-2	3.524	–	0.6	320
1.19	3.6E-2	3.522	–	0.6	345
1.2	2.2E-2	3.520	–	0.6	355
1.21	1.3E-2	3.518	–	0.6	380
1.22	8.2E-3	3.517	–	0.6	390
1.23	4.7E-3	3.515	–	0.6	405
1.24	2.4E-3	3.513	–	0.6	410
1.25	1.0E-3	3.511	–	0.6	430
1.26	3.6E-4	3.509	–	0.6	440
1.27	2.0E-4	3.508	–	0.6	455
1.28	1.2E-4	3.506	–	0.6	470
1.29	7.1E-5	3.505	–	0.6	500
1.3	4.5E-5	3.503	–	0.6	525
1.31	2.7E-5	3.502	–	0.6	550
1.32	1.6E-5	3.500	–	0.6	580
1.33	8.0E-6	3.499	–	0.6	610
1.34	3.5E-6	3.497	–	0.6	650
1.35	1.7E-6	3.496	–	0.6	670
1.36	9.5E-7	3.495	–	0.6	675
1.37	6.0E-7	3.494	–	0.6	680
1.38	3.8E-7	3.492	–	0.6	685
1.39	2.3E-7	3.491	–	0.6	690
1.4	1.4E-7	3.490	–	0.6	700
1.41	8.5E-8	3.489	–	0.6	710

Table 1 (continued)

λ (μm)	α (/cm)	n	k	C_n ($10^{-4}/\text{K}$) ($1/n$) (dn/dT)	$C_{k,\alpha}$ ($10^{-4}/\text{K}$) ($1/k$) (dk/dT)
1.42	5.0E-8	3.488	–	0.6	720
1.43	2.5E-8	3.487	–	0.6	730
1.44	1.8E-8	3.486	–	0.6	740
1.45	1.2E-8	3.485	–	0.6	750

Tabulated as a function of wavelength λ are the absorption coefficient α , the real and negative imaginary parts of the refractive index, n and k , and corresponding T coefficients (α has an identical coefficient to k). T coefficients are best used with Eqs. (9) and (10) of text. The tabulated free-space wavelength can be converted to energy by dividing 1.23984190 by the tabulated λ value (μm).

3. Data selection

A baseline tabulation of R versus E was prepared over abutting E ranges using different data sources and then a multiplier applied to give a final R value taking into account all available data. For example, Herzinger et al. [4] published an extensive tabulation used in the present work to calculate the R baseline over the 1–6 eV range. These data were then adjusted by taking into account other results over this range [13–15]. The consistency of these data meant that the multiplier applied to the baseline was within 0.2% of unity over most of this range. Below 1 eV, following Smith et al. [5–7], refractive index data judged most reliable [18–21] were corrected to 300K and plotted versus E squared, allowing fitting by the following expression (derived from Kramers–Kronig analysis, noting the low α below the Si band edge [3]):

$$n = 3.4164 + 0.085818E^2 + 0.010149E^4 \quad (4)$$

with E in eV (coefficients differ slightly from those of Smith et al. [5,7] since early data of Briggs [22] were rejected, while Primak's better quality data [20], incorrectly plotted in the earlier work, were included apart from 3 outliers). Eq. (4) was assumed valid to zero energy (free carrier and lattice absorption calculated to have negligible effect). Calculated R using this equation was only 0.013% lower than the 1–6 eV baseline value at 1 eV. The two data sets were merged over the 0.8–1.5 eV range using appropriate multipliers, with most of the small difference absorbed in the 1–6 eV baseline.

From 6–20 eV, the published reflectance curve of Philipp [14] was used, as recalculated from n and k values tabulated by Aspnes [23]. Also considered were data from Hunter [24], also tabulated by Aspnes [23]. From 20–29 eV, Hunter's data formed the baseline and the extensive tabulation of Henke et al. [25] was used from 29–30 keV (updated by results of Soufli and Gullikson [26]). Above 30 keV, a power law fit over the 20–30 keV range was projected [R (%) = $(E/E_0)^{-4.013}$, where $E_0 = 50.17$ eV].

4. Results

Fitted reflectance at 300K is shown in Fig. 1(a), together with a selection of data taken into account. Below the bandgap, θ should be zero. With a sensible fit to R , calculated θ at 1 eV was -0.0007 rad, small but physically impossible. This shows all R data, not surprisingly, were not 100% accurate. While accurate to much better than 1% below 5.8 eV, larger errors were expected above this energy. To offset this error in a tractable way, a multiplier of 0.945 was applied to data above 29 eV. This reduced θ at 0.85, 1 and 1.16 eV to a physically more realistic 0 ± 0.00008 rad. From Eq. (3), this corresponds to an uncertainty of ± 0.0004 in k at these energies. The previous adjustment is equivalent to assuming a 5.5%

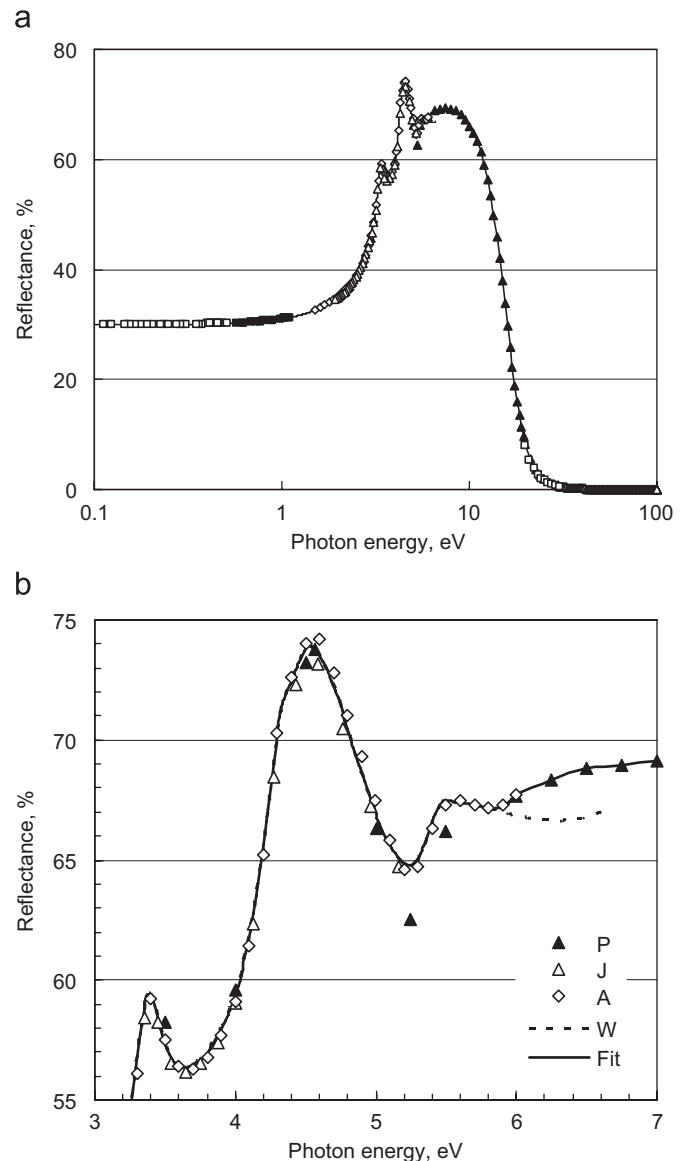


Fig. 1. (a) Silicon reflectance, R , from a selection of data sources used in this work together with the fit used in the present analysis (solid line); (b) Reflectance over the 3–7 eV range, showing final fit (solid line) and the data used in determining this fit (closed triangles, Philipp [16]; open triangles, Jellison [13]; open diamonds, Aspnes and Studna [15]; dashed line, mostly obscured, Herzinger et al. [4]).

error in the integral

$$\theta_h = -\frac{29 \text{ eV}}{\pi} \int_{29 \text{ eV}}^{\infty} \frac{\ln(R)}{E^2} dE \quad (5)$$

Although related integrals over this E range are known reasonably accurately (such as integrals giving effective carriers involved in absorption), the integral in Eq. (5) could well be in error by this amount [7].

Fig. 1(b) shows R versus E from 3 to 7 eV, showing more clearly the range of data taken into account, and the final R fit (adjustments to 300 K also incorporated). Calculated n and k , listed in Table 1, show a similar E dependence to those plotted elsewhere [13], although differing in detail. At λ above $0.5 \mu\text{m}$ (E below 2.5 eV), k could be calculated more accurately from measured α . At such wavelengths, k was calculated from α , with n then calculated from k and the fitted R . Good agreement was obtained from $0.46\text{--}0.6 \mu\text{m}$ between the n , k and α values deduced from the two approaches. The α measurements of Weakliem and Redfield [27], MacFarlane et al. [28], Keevers and Green [29], Trupke et al. [10] and Reece et al. [30] were given highest weighting from 0.47 to $1.45 \mu\text{m}$.

5. Accuracy

Error limits on tabulated k and α are estimated to increase from $\pm 0.3\%$ at $0.25 \mu\text{m}$ to $\pm 4\%$ beyond $0.46 \mu\text{m}$, $\pm 10\%$ beyond $1.2 \mu\text{m}$ and to become even larger beyond $1.4 \mu\text{m}$. For n , estimated accuracy is better than $\pm 0.1\%$ beyond $1.0 \mu\text{m}$, increasing to about $\pm 0.5\%$ at shorter λ except below $0.3 \mu\text{m}$ where it increases to $\pm 1\%$. An earlier survey [3] identified two laser wavelengths, where accurate n and k values were known. Extrapolated to 300 K, the complex index of Taft [31], $(4.088 \pm 0.003) - i(0.0314 \pm 0.0016)$ at 546.1 nm , is highly regarded [3,15] as is Geist's value [3], $3.874 - i(0.0159 \pm 0.0004)$ at 633.0 nm . The present values, $(4.090 \pm 0.003) - i(0.0289 \pm 0.0012)$ and $(3.874 \pm 0.002) - i(0.0162 \pm 0.0006)$, respectively, are self-consistent with k at the lower side of Taft's range and the upper side of Geist's.

A very sensitive check at the high energy (short wavelength) end of the spectrum is provided by the value of the imaginary part of the dielectric function ($= 2nk$) at an energy close to 4.25 eV (292 nm) where this parameter has a strong peak [31]. The highest reported value at the peak appears to be 48.3 ± 1.0 at nominally room temperature for H terminated, $\langle 111 \rangle$ orientated silicon wafers [31]. By way of comparison, Herzinger et al. [4] report a peak room temperature value of 47.7 for oxide terminated $\langle 100 \rangle$ wafers (no error estimates). Jellison [13] similarly measures values of 46.5 ± 0.6 , 47.5 ± 0.6 and 46.8 ± 0.6 for $\langle 100 \rangle$, $\langle 111 \rangle$ and $\langle 110 \rangle$ wafers. He attributes the differences to different surface reconstructions or surface strains beneath the thin thermal oxides present ($0.6\text{--}0.8 \text{ nm}$ thick), with the optical effect of these oxide layers taken into account in the data extraction. A reasonably representative value based on the above data would be 47.7 ± 1.0 , the value of Herzinger et al. [4] with the error estimate deduced from the scatter in the above results, attributed primarily to different surface terminations.

At 290 nm and 300 K , the Herzinger et al. [4] data set and transferred error estimate gives 46.2 ± 1.0 . The tabulated values of n and k correspond to 46.1 ± 0.9 , in the middle of the uncertainty range, an excellent choice for general purpose use. At the other extreme of very low energy, the work of Gatesman [17] provides an n value of 3.4170 ± 0.0001 and $k \leq 0.0001$ at $\lambda = 236.6 \mu\text{m}$. The n value deduced by the present methodology corrected to standard room temperature (22°C) is only 0.04% lower. Accordingly error estimates appear reasonable across the whole range of tabulated values.

6. Temperature dependency

Also given in Table 1 is the normalised temperature coefficient of the optical constants calculated from cited and additional data

sets [32], defined as

$$c_p = \frac{1}{p} \frac{dp}{dT} = \frac{d(\ln p)}{dT} \quad (6)$$

where p is the property of interest (n , k or α). Of two equally valid ways to use this coefficient suggested by Eq. (6), the simplest is

$$p(T_o + \Delta T) = p(T_o)(1 + c_p \Delta T) \quad (7)$$

An equally general alternative is

$$p(T_o + \Delta T) = p(T_o) \exp(c_p \Delta T) \quad (8)$$

Eq. (8) might be appropriate for parameters that vary over wide ranges with T and which never become negative, as for n and k . A third and more preferred expression is based on the observation [33] that α at 1064.1 nm follows the power law

$$p(T) = p(T_o)(T/T_o)^b \quad (9)$$

with T in Kelvin and b a constant at fixed λ ($b = 4.25$ at 1064.1 nm [33]). Data of Weakliem and Redfield [27], in particular, show similar power law relationships are obeyed over a wide λ range ($0.46\text{--}1.26 \mu\text{m}$). Basic calculus gives

$$b = C_p(T)T = C_p(T_o)T_o \quad (10)$$

Hence, b can be found from the tabulated T coefficients and Eq. (9) used for extrapolation. This approach has the advantage that it incorporates the experimental T dependence of the T coefficient. Accuracy is demonstrated in Fig. 2, showing the tabulated α data extrapolated using Eqs. (9) and (10) to 249 , 363 and 473 K , temperatures where α is known most accurately [10,27,28]. Extrapolation using Eq. (8) produced almost identical results at 294 and 363 K but overestimated values at 473 K , while Eq. (7) gave poor results at long λ . Although extrapolation misses details such as smearing of phonon features at high T and cannot accurately model T shifts of phonon and bandgap energies, agreement between extrapolated and experimental data is excellent. Even at the three selected T , extrapolated values are more accurate than available experimental data at some energies. At other temperatures, this could well be the case over the entire energy range.

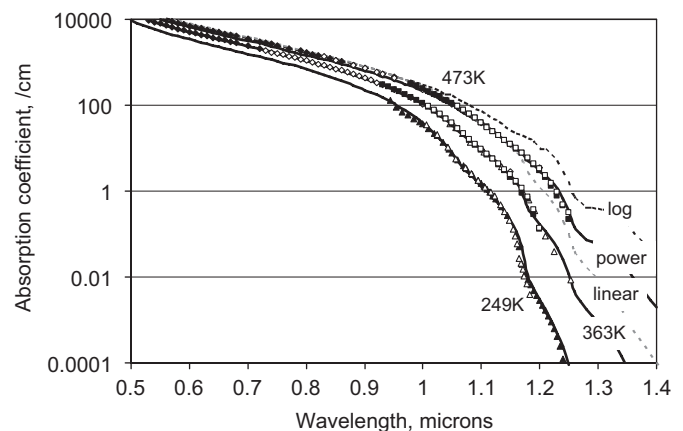


Fig. 2. Silicon absorption coefficient, α , as a function of wavelength, λ , with temperature as the parameter. The solid lines show α at 249 , 363 and 473 K extrapolated from 300 K using the tabulated temperature coefficients and Eqs. (9) and (10) of the text. The dashed lines show the extrapolated value at 473 K using Eq. (7) "linear" and (8) "log" of text. Also shown are the best experimental values at these temperatures (open triangles, MacFarlane et al. [28]; closed triangles, Trupke et al. [10]; open and closed squares and diamonds, four different thickness samples of Weakliem and Redfield [27]).

Acknowledgements

The author gratefully thanks H.A. Weakliem for providing tabulations of his published data and G.E. Jellison Jr., T. Trupke, P. Reece, C.M. Herzinger, D.Y. Smith, W. Karstens and M. Inokuti for providing access to additional data. This work was supported by the Australian Research Council. He thanks Marc Rüdiger, Thorsten Trupke and unidentified referees for comments on the manuscript.

References

- [1] M.A. Green, High Efficiency Silicon Solar Cells, Trans Tech Publications, Aedermannsdorf, 1987 Appendix C, pp. 228–231.
- [2] M.A. Green, M.J. Keevers, Optical Properties of Intrinsic Silicon at 300 K, Progr. Photovoltaics 3 (1995) 189.
- [3] J. Geist, Silicon revisited, in: E.D. Palik (Ed.), Handbook of Optical Constants of Solids III, Academic Press, New York, 1998, pp. 519–529.
- [4] C.M. Herzinger, B. Johs, W.A. McGahan, J.A. Woollam, Ellipsometric determination of optical constants for silicon and thermally grown silicon dioxide via a multi-sample, multi-wavelength, multi-angle investigation, J. Appl. Phys. 83 (1998) 3323.
- [5] D.Y. Smith, M. Inokuti, W. Karstens, Photoresponse of condensed matter over the entire range of excitation energies: analysis of silicon, Phys. Essays 13 (2–3) (2000) 465.
- [6] D.Y. Smith, M. Inokuti, W. Karstens, A generalized Cauchy dispersion formula and the refractivity of elemental semiconductors, J. Phys.: Condens. Matter 13 (2001) 3883.
- [7] E.J. Shiles, M. Inokuti, W. Karstens, D.Y. Smith, Surface Effects and UV Optical Properties of Silicon, APS Presentation, March Meeting, 2003.
- [8] M.A. Green, J. Zhao, A. Wang, P.J. Reece, M. Gal, Efficient silicon light emitting diodes, Nature 412 (2001) 805.
- [9] E. Daub, P. Würfel, Ultralow values of the absorption-coefficient of Si obtained from luminescence, Phys. Rev. Lett. 74 (1995) 1020.
- [10] T. Trupke, M.A. Green, P. Würfel, P.P. Altermatt, A. Wang, J. Zhao, R. Corkish, Temperature dependence of the radiative recombination coefficient of intrinsic crystalline silicon, J. Appl. Phys. 94 (2003) 4930.
- [11] P.J. Mohr, B.N. Taylor, CODATA recommended values of the fundamental physical constants: 2002, Rev. Mod. Phys. 77 (2005) 1.
- [12] K.P. Birch, M.J. Downs, Correction to the updated Edlen equation for the refractive index of air, Metrologia 31 (1994) 315.
- [13] G.E. Jellison Jr., Optical functions of silicon determined by two-channel polarization modulation ellipsometry, Opt. Mater. 1 (1992) 41.
- [14] H.R. Philipp, Influence of oxide layers on the determination of the optical properties of silicon, J. Appl. Phys. 43 (1972) 2835.
- [15] D.E. Aspnes, A.A. Studna, Dielectric functions and optical parameters of Si, Ge, GaP, GaAs, GaSb, InP, InAs, and InSb from 1.5–6.0 eV, Phys. Rev. B 27 (1983) 985.
- [16] K.W. Boer, Survey of Semiconductor Physics, second ed., Wiley, New York, 2002, p.505.
- [17] A.J. Gatesman, A High Precision Reflectometer for the Study of Optical Properties of Materials in the Submillimeter, University of Lowell, Lowell, Massachusetts, 1993 Ph.D. Thesis.
- [18] C.D. Salzberg, J.J. Villa, Infrared refractive indices of silicon, germanium and modified selenium glass, J. Opt. Soc. Am. 47 (1957) 244.
- [19] F. Lukes, The temperature-dependence of the refractive index of silicon, J. Phys. Chem. Solids 11 (1959) 342.
- [20] W. Primak, Refractive index of silicon, Appl. Opt. 10 (1971) 759.
- [21] H.W. Icenogle, B.C. Platt, W.L. Wolfe, Refractive indices and temperature coefficients of germanium and silicon, Appl. Opt. 15 (1976) 2348.
- [22] H.R. Briggs, Optical effects in bulk silicon and germanium, Phys. Rev. 77 (1950) 287.
- [23] D.E. Aspnes, Optical Functions of Intrinsic Si, in Properties of Silicon, INSPEC, IEE, London, 1988, p. 72.
- [24] W.R. Hunter, As listed in several references [21,23] but possibly originally, in: F. Abels (Ed.), Optical Properties and Electronic Structure of Metals and Alloys, North-Holland, Amsterdam, 1966, p. 136.
- [25] B.L. Henke, E.M. Gullikson, J.C. Davis, X-ray interactions: photoabsorption, scattering, transmission, and reflection at $E = 50\text{--}30,000$ eV, $Z = 1\text{--}92$, A. Data Nucl. Data Tables 54 (1993) 181 (updated tabulation at www-cxro.lbl.gov/optical_constants/asf.html).
- [26] R. Soufli, E.M. Gullikson, Reflectance measurements on clean surfaces for the determination of optical constants of silicon in the extreme ultraviolet-soft-X-ray region, Appl. Opt. 36 (1987) 5499.
- [27] H.A. Weakliem, D. Redfield, Temperature dependence of the optical properties of silicon, J. Appl. Phys. 50 (1979) 1491.
- [28] G.G. MacFarlane, T.P. McLean, J.E. Quarrington, V. Roberts, Fine structure in the absorption-edge spectrum of Si, Phys. Rev. 111 (1958) 1245.
- [29] M. Keevers, M.A. Green, The absorption edge of silicon from solar cell spectral response measurements, Appl. Phys. Lett. 66 (1995) 174.
- [30] P.J. Reece, M.A. Green, J. Zhao, A. Wang, M. Gal, unpublished work, 2001.
- [31] E.A. Taft, The optical constants of silicon and dry oxygen oxides of silicon at 5461 Å, J. Electrochem. Soc. 125 (1978) 968.
- [32] G.E. Jellison Jr., F.A. Modine, Optical functions of silicon at elevated temperatures, J. Appl. Phys. 78 (1994) 3758.
- [33] K.G. Svantesson, N.G. Nilsson, Determination of the temperature dependence of the free carrier and interband absorption in silicon at 1.06 μm , J. Phys. C: Solid State Phys. 12 (1979) 3837.